Published in Chemical Engineering Science 2013

Binary and ternary VLE of the 2-(diethylamino)-ethanol (DEEA)/ 3-(Methylamino)-propylamine (MAPA)/ Water system

*Ardi Hartono[a], Fahad Saleem[a], Muhammad Waseem Arshad[b], Muhammad Usman[a] and Hallvard F. Svendsen[a]**

[a]*Department of Chemical Engineering, Norwegian University of Science and Technology, N-7491 Trondheim, Norway*

[b]*Technical University of Denmark, Søltofts Plads,2800 Lyngby, Denmark*

** To whom correspondence should be addressed, Phone: +47-73594100, Fax: +47-73594080, e-mail: hallvard.svendsen@chemeng.ntnu.no*

Keywords: VLE, Alkalinity, DEEA, MAPA, Absorption, Modeling

Abstract

A mixed 2-(Diethylamino)-ethanol (DEEA) and 3-Methylamino)-propylamine (MAPA) system could be an attractive alternative solvent to improve the performance of CO_2 capture for low partial pressure cases. This solvent has the advantages of forming two liquid phases upon CO_2 loading, one rich in CO_2 and the other very low in CO_2. Having a highly concentrated rich solvent improvements could be

reached by reducing the sensible heat and improving the equilibrium sensitivity hence reducing the need for stripping steam. Also it is possible that the heat of absorption may change to the better.

To better understand this system in designing the separation unit requires substantial work on characterization of the solvent. One important aspect is to provide equilibrium data. In this work new ebulliometric VLE data for the binary DEEA/H_2O and DEEA/MAPA systems and the ternary DEEA/MAPA/H_2O system are reported at different temperatures and concentrations. Results show that pure MAPA is more volatile than DEEA, but in aqueous solution MAPA was found to be less volatile. A mix of DEEA and MAPA in aqueous solution tends to lower the volatility thus makes the system more advantageous by reducing volatility. The activity coefficients for the species in the ternary aqueous system are found to be lower than the activity coefficients obtained from the corresponding binary aqueous mixtures.

The UNIQUAC framework was implemented to represent the experimental data. The six UNIQUAC parameters were determined and were able to predict P-T-x-y, activity coefficient, excess enthalpy and freezing point depression for both the binary and ternary systems. However, a small inconsistency was observed between water activity coefficients determined from ebulliometer and freezing point depression measurements

1. Introduction

Amine mixtures which potentially form two phases at higher CO_2 concentration have recently received attention as a CCS technology. The changes in technology comprises two major elements, solvent and process development. When two phases occur the regeneration heat requirement could be expected to be lower as only a lower phase, being a highly concentrated rich solvent is sent to the stripper and the sensible heat loss could be reduced. By forming a second phase the equilibrium temperature sensitivity could be improved thereby reducing the need for stripping steam and also the heat of absorption may be affected positively.

The DMX process by IFPEN is based on special solvents forming two immiscible phases and is now under testing in Italy (Raynal, et al., 2011). This process is claimed to give a specific reboiler duty as

low as 2.1 GJ/tonne CO_2 captured which is significantly lower than the 3.0-3.7 GJ/t CO_2 reported for the modified and classical 30wt% MEA reference processes. Another process with two liquid phases is based on a thermomorphic biphasic solvent type. It gives a single phase at lower temperature but two phases at higher temperature (Zhang, et al., 2011). The advantage of this solvent was to adopt it to a concept where regeneration of the solvent can take place without steam.

A blend of 2-(Diethylamino)-ethanol (DEEA) and 3-Methylamino)-propylamine (MAPA) having characteristics of a biphasic/phase change solvent is now intensively studied at NTNU within the EU iCap project. At very low CO_2 loadings, this solvent behaves as a single phase but at higher CO_2 loadings it gives two phases. For design and modeling of this gas treating process the knowledge of vapor–liquid equilibrium (VLE) of the mixed amine/CO_2/water system is required. At low CO_2 gas concentrations the phase equilibrium is governed by the binary/ternary DEEA/MAPA/water system.

DEEA is a tertiary alkanolamine, which has received interest by different researchers both as pure and in aqueous solution. Among data available are heat of reaction of CO_2 (Kim, 2009), freezing point depression (Arshad, et al., 2013), kinetic absorption CO_2 rate (Konduru, et al., 2010; Vaidya and Kenig, 2009), viscosity (Maham, et al., 2002), density (Lebrette, et al., 2002), excess enthalpy (Mathonat, et al., 1997) and vapor pressure (Klepáčová, et al., 2011; Kapteina, et al., 2005; Steele, et al., 2002).

MAPA is diamine which has one primary and one secondary amine group attached. It would be expected to have fast absorption kinetics. Reports on characterization of MAPA both as pure and in aqueous solution are limited. Data available are: heat of reaction of CO_2 (Kim, 2009), vapor pressure and binary aqueous MAPA VLE data where two different thermodynamic models were developed, i.e. Wilson and NRTL (Kim, et el., 2008). Aronu (2011) implemented the UNIQUAC model to these data. Other data are freezing point depression (Arshad, et al., 2013) and vapor pressure of MAPA at very low concentrations (Nguyen, et al., 2011). No experimental data and thermodynamic model could be found for the binary DEEA/MAPA and ternary of DEEA/MAPA/H_2O systems.

In this work, we report a set of new experimental data on the binary systems DEEA/H_2O and DEEA/MAPA as well as ternary VLE data for the DEEA/MAPA/H_2O system based on ebulliometer

measurements. The gathered P-T-x-y data were modeled with a UNIQUAC thermodynamic model to determine the binary interaction parameters.

2. Experimental Section

2.1. Material

Reagent grade 2-(diethylamino)-ethanol (DEEA) with purity > 99.5% and 3-(Methylamino)-propylamine (MAPA) with purity > 98.5 % supplied by Sigma-Aldrich were used without further purification. The solutions were prepared gravimetrically by dissolving the chemicals in deionized water.

2.2. Vapor pressure measurements of pure DEEA(1) and pure MAPA(2)

The P-T vapor pressure data for pure solvents at different temperatures were measured in a modified Swietoslawski ebulliometer apparatus (Hartono, et al., 2013; Kim, et al., 2008). The measurements were started at ambient pressure to measure normal boiling point and then the pressure was reduced to generate data at lower temperatures.

2.3. Binary VLE measurements of the DEEA(1)+H_2O(3) and DEEA(1)+MAPA(2) systems

P-T-x-y data for the binary system DEEA/H_2O at different temperatures and concentrations were measured in the same apparatus. A gravimetrically prepared, 80 weight % solution of DEEA in water was initially fed to the ebulliometer. During the experiment, after each equilibration, the initial solution was diluted gradually to achieve high dilution at the end. While for MAPA/H_2O, the reported data (Kim et al., 2008) were collected and used.

P-T-x-y data of DEEA/MAPA system were also measured. By feeding pure DEEA or MAPA into the apparatus and diluting gradually with MAPA or DEEA to achieve high dilution at the end. The binary interaction parameters between the two amines could then be determined. This work was easy compared to the previous AMP/Pz system (Hartono, et al., 2013), since both of the amines were in liquid state. Detailed experimental procedures can be found in previous work (Hartono, et al., 2013; Kim et al., 2008).

2.4. Ternary VLE measurements of DEEA(1)+MAPA(2)+H_2O(3) system

Eight different concentrations of ternary DEEA/MAPA/H_2O solutions were prepared gravimetrically. They provided different mole ratios of DEEA/MAPA (0.20, 0.25, 0.40, 0.50, 2.0, 2.5, 4.0, and 5.0) and were individually fed into the ebulliometer. When equilibrium was established at a specific temperature, samples of liquid and vapor phase were collected. Each ratio of DEEA/MAPA was completed in one run from the lowest to the highest possible temperature.

2.5. Liquid (x) and vapor (y) phase analyses

The collected liquid and vapor solutions were examined with amine titration (Mettler Toledo G20) to determine the amine concentrations for the binary systems. High concentration samples were analyzed with 0.2N H_2SO_4 as titrant but for the low concentration samples 0.02N H_2SO_4 had to be used. The end point of each titration curve was used to calculate the concentration of amine according to eq. 1.

For the binary DEEA/MAPA system, the concentration of each amine was estimated from the total alkalinity according to:

$$Alk\left(\frac{mol}{kg_{Solution}}\right) = \frac{2\times(M\times V)_{H_2SO_4}}{w_{sample}} \qquad (1)$$

$$x_1 = \frac{(Alk\times M_2 - n_2)}{(n_1 - Alk\times M_1)}\times x_2 \qquad (2)$$

$$x_1 + x_2 = 1 \qquad (3)$$

For the ternary DEEA/MAPA/H_2O system, two parallel samples were analysed with Liquid Chromatography-Mass Spectroscopy (LCMS) to quantify the concentration of each compound. The LC-MS analyzes were performed on an LC–MS/MS system, 6460 Triple Quadrupole Mass Spectrometer coupled with 1290 Infinity LC Chromatograph and Infinity Autosampler 1200 Series G4226A from the supplier Agilent Technologies. The same technique was implemented for different amines/ alkanolamines and details regarding procedures can be found in previous works (Vevelstad, et al., 2013; da Silva, et al., 2012; Lepaumier, et al., 2011). The reported concentrations were on volumetric base and to quantify each amine on the gravimetric basis the total alkalinities (Alk), (Eq. 1) were measured by

titration and the results from the LCMS were used as the mole ratio DEEA/MAPA (h). Hence the concentrations of DEEA and MAPA were calculated according to:

$$x_1 = \frac{h}{1+h} \times Alk \qquad (4)$$

$$x_2 = \frac{1}{1+h} \times Alk \qquad (5)$$

$$x_1 + x_2 + x_3 = 1 \qquad (6)$$

2.5. Source of uncertainty

Minor uncertainty sources were from pressure $(\mathrm{D}P \pm 0.3 kPa)$ and temperature $(\mathrm{D}T \pm 0.05 K)$ (Kim, et al., 2008). However, the liquid and vapor phase analyses play a very important role in the calculation of activity coefficients and are the main source of uncertainty.

The titration analysis for alkalinity gives a deviation between two parallel samples typically less than 1%. The LCMS method reports an average deviation estimated to about 3%. The maximum propagation error (Ku, 1966) was estimated for the alkalinity measurement $(\mathrm{D}Alk \pm 1\%)$ and for concentration $(\mathrm{D}x \pm 3\%)$.

3. Determination of experimental activity coefficient (g_i^{Exp})

The ebulliometer experiments can usually provide P-T-x-y data for both binary and ternary systems and the experimental activity coefficients (g_i^{Exp}) for each amine were determined according to Eq. 7 (Van Ness, 1995)

$$g_i^{Exp} = \frac{y_i \times P}{x_i \times P_i^{\circ}} \times \mathrm{F}_i \qquad (7)$$

Here x_i, y_i, P, P_i° and F_i are liquid mole fraction, vapor mole fraction, total pressure of solution, saturation pressure of pure substance, and the Poynting factor respectively. Eq. 7 is developed for molecular systems and no hydrolysis of amine is taken into account as the amine itself is the main

contributor in the speciation. A detailed discussion on the hydrolysis effect can be found in previous work (Hartono, et al., 2013).

4. The activity coefficient model (g_i^{calc})

The UNIQUAC thermodynamic model (Abrams and Prausnitz, 1974) was used to interpret the data. It requires 6 parameters to be determined, i.e. the van der Waals volume parameter (r), area parameter (q), and interaction energy parameter (u_{ij}^0, u_{ij}^T) for each binary system.

The available excess enthalpy of solution (H^E) was included in the model prediction. The derivation of the excess enthalpy for the UNIQUAC model (Thomsen, 1999) was implemented and the freezing point depression was estimated with the method developed by Ge and Wang (2009).

5. Regression

The 6 parameters of the UNIQUAC model were determined by using an in-house Matlab code for multi-response parameter estimation, *Modfit* (Hertzberg and Mejdell, 1998), with an objective function (F)as given by Eq. 8.

$$F = \sum_{i=1}^{n} \left(\frac{g_{\text{Amine}}^{Exp} - g_{\text{Amine}}^{calc}}{g_{\text{Amine}}^{Exp}} \right)^2 + \sum_{i=1}^{n} \left(\frac{P_{\text{Sol}}^{Exp} - P_{\text{Sol}}^{calc}}{P_{\text{Amine}}^{Exp}} \right)^2 + \sum_{i=1}^{n} \left(\frac{(H_{\text{Sol}}^{E})^{Exp} - (H_{\text{Sol}}^{E})^{calc}}{(H_{\text{Sol}}^{E})^{Exp}} \right)^2 + \sum_{i=1}^{n} \left(\frac{(Q_{Sol}^{F})^{Exp} - (Q_{Sol}^{F})^{calc}}{(Q_{Sol}^{F})^{Exp}} \right)^2 \quad (8)$$

Deviations between model results and experimental data were expressed as absolute average relative deviations (AARD) according to Eq. 9.

$$AARD = \frac{1}{n} \sum_{i=1}^{n} \frac{\left| W_{\text{model}} - W_{\text{exp}} \right|}{W_{\text{exp}}} \quad (9)$$

where W would be the activity coefficient, total pressure of solution, excess enthalpy and freezing point depression, respectively.

Experimental activity coefficients for the DEEA/H_2O, DEEA/MAPA and DEEA/MAPA/H_2O (g_i^{Exp}) systems are reported in this work while data for the MAPA/H_2O system were taken from earlier work (Kim, et al., 2008). Available total pressure of solution (P_{Sol}^{Exp}), excess enthalpy (H_{Sol}^{E}) and freezing point depression (Q_{Sol}^{F}) data were taken from the literature. For the DEEA/H_2O system all three selected responses were available in the literature but for the MAPA system only the VLE data and the freezing point depression (Q_{Sol}^{F}) were found.

6. Results and Discussion

6.1. Vapor pressure of pure Solvent (DEEA and MAPA)

The saturation pressures of pure solvents were measured at different temperatures and the results are summarized in an Appendix (Table A.1. and Table A.2.). An Antoine equation (Antoine, 1888) was used to represent the data in Fig. 1. It is seen that MAPA is more volatile than DEEA due to the absence of alcohol group in its molecular structure. The vapor pressure of MAPA in this work agrees very well with literature data (Kim, et al., 2008) while for the vapor pressure of DEEA a small discrepancy with literature data is observed. The data sets for DEEA, including data from the literature, cover a wide range of temperatures (5-203^{o}C) while for MAPA the range is only 54-139^{o}C. However, an extrapolation of the data to lower temperatures could be done with good accuracy. The obtained three parameters of the Antoine equation are shown in Table 1 along with the average absolute relative deviation (AARD) between model and data.

Table 1. Antoine equation and the obtained parameters for pure DEEA and MAPA

Figure 1. Saturation pressures of pure DEEA and MAPA

6.1. Binary VLE of the DEEA(1)+H_2O(3) system

VLE for the DEEA/H_2O system were measured in the ebulliometer for four temperatures (40, 60, 80 and 95^{o}C) and the results are shown in an Appendix (Table A.3). DEEA is a derivate of MEA with two

ethyl groups substituted for two protons. This substitution increases the volatility of DEEA compared to MEA, as can be seen in the k-values and the activity coefficients respectively.

The increase in k-value with temperature indicates that the volatility of DEEA increases more than that of water, while its decrease with concentration shows that the activity coefficient decreases. When the k-value of DEEA is compared with MEA at the same concentration and temperature (Kim, et al., 2008), it is found that DEEA is more volatile as expected.

The collected experimental data for P-T-x-y (this work), excess enthalpy (Mathonat, et al., 1997) and freezing point depression (Arshad, et al., 2013) were regressed according to eq. 8. The obtained UNIQUAC volume (r) and surface area (q) parameters are tabulated in Table 2 while the UNIQUAC interaction energy parameters are shown in Tables 3 and 4. The AARD values are given in Table 5.

Table 2. Volume (r) and surface area (q) parameters for the selected systems

Table 3. UNIQUAC interaction energy parameters for $u_{ij} = u_{ij}^{\circ} + u_{ij}^{T} \times (T - 298.15); u_{ij}^{\circ} = u_{ji}^{\circ}$

Table 4. UNIQUAC interaction energy parameters for $u_{ij} = u_{ij}^{\circ} + u_{ij}^{T} \times (T - 298.15); u_{ij}^{T} = u_{ji}^{T}$

Table 5. Absolute average relative deviations (AARD) of model for DEEA(1)+H_2O(3), MAPA(2)+H_2O(3) and DEEA(1)+MAPA(2) .

Comparisons of the experimental activity coefficients (g_i^{Exp}) of DEEA in Fig. 2 and MEA at low concentrations $(x_1 \leq 0.2)$ shows that DEEA has values from 20 to 1.5 while MEA has low values in the range 0.2-0.5 (Kim, et al., 2008). Thus DEEA is in particular more volatile than MEA but the activity coefficient decreases with concentration contrary to MEA where the activity coefficient increases with concentration.

Figure 2. Experimental and predicted activity coefficients for DEEA and water at different concentrations

Fig. 3 shows that the model is able to represent the P-T-x-y data very well and it is observed that the mixture of DEEA and water exhibits an azeotrope at very low concentrations $(x_1 < 0.1)$. The azeotrope point is found to shift to higher concentrations with increasing temperature.

Figure 3. Experimental P-T-x-y data at different temperatures compared with model predictions

The reported excess enthalpy of DEEA solutions (Mathonat, et al., 1997) and freezing point data (Arshad, et al., 2013) were also used in the parameter estimation as shown in Fig. 4 and Fig. 5. The model gives a reasonably good representation of the excess enthalpy data. However, a shift in the minimum excess enthalpy value is observed when both the excess enthalpy and freezing point data are taken into account in the regression. No significant effect in the total pressure and activity coefficient predictions is seen. This behavior was also observed in previous work on AMP/H_2O (Hartono, et al., 2013) and MEA/H_2O (Aronu, et al., 2011).

Figure 4. Experimental excess enthalpy of DEEA solutions compared to model predictions at 25^{o}C

The activity coefficient of water in the solution can be estimated both from the freezing point depression (SLE) data and the ebulliometric measurements (VLE). When both data are taken into account into the parameter regression a discrepancy appears at higher concentrations and lower temperatures. This problem might be explained by extrapolation of ebulliometer data down to very low temperatures, as the range for typical freezing point depression measurements, could be uncertain.

Figure 5. Experimental freezing point depression of DEEA solution and the predicted model

6.2. Binary MAPA(2)+H_2O(3) system

Only the reported VLE for the binary MAPA/H_2O system (Kim, et al., 2008) and the freezing point depression data (Arshad, et al., 2013) were used in the regression to determine the UNIQUAC parameters as shown previously in Tables 2, 3 and 4 along with the AARD value in Table 5. The reported volume (r) and area (q) regressed in this work are lower than those found by Aronu (2011). This may be explained by the obtained parameters from previous work were only regressed from VLE data.

The representation of the model for activity coefficients of MAPA and water are shown in Fig. 6. MAPA has lower activity coefficients than MEA (Kim, et al., 2008) and of the same order of magnitude as Pz (Hartono, et al., 2013). Even though MAPA does not have any hydroxyl/alcohol group MAPA become much less volatile in water solution. In general the agreement between model and experimental

data is good, Fig. 6 and Fig. 7. The apparent inconsistency of the model at low MAPA concentration ($x_2 < 0.03$) at 80°C can be attributed to uncertainties in the experiment itself while at high concentration ($x_2 > 0.25$) a dilution technique was used (Kim, et al., 2008) which was reported as an important source of uncertainty.

Figure 6. Experimental data (Kim, et al., 2008) and predicted activity coefficients for MAPA and water at different concentrations

An azeotropic behavior at low temperature (40°C) and high MAPA concentration ($0.7 < x_2 < 0.9$) is predicted by the model but cannot be verified due to lack of data.

Figure 7. Experimental P-T-x-y data at different temperatures and the predicted models

Reported vapor pressure data for MAPA at 0.5 m (mole MAPA/ kg water) at different temperatures (Nguyen, et al., 2011) were plotted together with model predictions in Fig. 8 and as seen the model predicts well at low temperature ($t < 50^{\circ}C$) but shows some over-prediction at higher temperatures. The discrepancy might be associated with uncertainty in the experimental data as also seen in the Pz/H_2O system (Hartono, et al., 2013).

Figure 8. MAPA vapor pressure at 0.5 molality (m) and 40-70°C

When no excess enthalpy data were used in the parameter regression a good prediction for freezing point depression was expected. However, as seen in Fig. 9 the model appears to over-predict the data at higher concentrations ($x_2 > 0.07$). This can be caused by extrapolation of ebulliometer data to low temperatures, as earlier mentioned, but could also indicate inconsistencies between the measured water activity coefficients from ebulliometer (VLE) and from the freezing point depression experiments (SLE).

Figure 9. Experimental freezing point depression of MAPA solution and the predicted model

6.3. Binary DEEA(1)+MAPA(2) system

Binary VLE measurements for blended pure DEEA and MAPA were conducted in this work at three temperatures (80, 100 and 120°C) and the results are shown in an Appendix (Table A.4.). The k-values

are found to have a minimum point in the middle range of DEEA concentrations. This indicates a trend in volatility of DEEA with increasing concentration: decreasing, reaching a minimum value and then increasing again. The temperature has no significant effect in shifting the minimum point in DEEA concentration. The k-value of DEEA in MAPA is lower than that in water suggesting that blending DEEA and MAPA could reduce the volatility in the system.

The binary interaction of DEEA/MAPA was regressed from the data (in Table A.4) for the activity coefficient and total pressure and the results were already shown in Table 3 and Table 4, along the AARD values in Table 5. The activity coefficients of DEEA in MAPA are found to be lower than those in water as seen in Fig. 10 where it varies in the range from 1.2 to 0.8 at 80^{o}C. The activity coefficients of MAPA in DEEA do not change significantly compared to the activity coefficients of MAPA in water. Temperature gives a slight increase of the DEEA activity coefficients but for MAPA the opposite is seen.

Figure 10. Experimental data and predicted activity coefficients for DEEA and MAPA at different concentrations

The P-T-x-y data are represented well by the model as seen in Fig. 11. However, at very high concentrations of DEEA the model shows an under-prediction of the experimental points but an over-prediction at the highest temperature in the middle concentration. This might be caused by uncertainties in the developed Antoine equation for pure DEEA from the collected experimental data (in Table A.1). An azeotrope is also observed in the high range of DEEA concentrations and slightly shifting down in concentration with increasing temperature.

Figure 11. Experimental P-T-x-y data for DEEA and MAPA at different temperatures and the predicted models

6.4. Ternary DEEA(1)+MAPA(2)+H_2O(3) system

The experimental results of the ternary VLE experiments at six different temperatures and eight different DEEA/MAPA ratios are collected in an Appendix (Table A.5.). Fig. 12 shows the k-values of DEEA and of MAPA in the ternary system are observed to be lower than that in the binary DEEA/H_2O

and MAPA/H_2O systems. This means that the volatility of DEEA is reduced in the presence of MAPA while for MAPA a similar trend is observed in the presence of DEEA at similar concentrations and temperatures.

Figure 12. Experimental and predicted k-values for DEEA(1) and MAPA(2) in the DEEA/MAPA/H_2O system at 40^oC (a), 50^oC (b), 60^oC (c), 80^oC (d), 100^oC (e) and 110^oC (f)

As seen in Fig. 13, the activity coefficients of DEEA are found to be lower in the ternary system than in the binary system. This also goes for MAPA. The solid and dashed lines are generated respectively with and without the binary interaction of DEEA/MAPA taken into account. It is clearly seen that at similar temperature and concentration the activity coefficients in the ternary system are lower than those of the binary systems as it was also show previously with the k-values. For AMP/Pz/H_2O (Hartono, et al., 2013) and other systems (Kim, 2009) it was stated that the activity coefficients for the species in the ternary system are in general similar to the activity coefficients obtained from the corresponding binary mixtures, however this is not the case for the DEEA/MAPA system. The binary interaction parameters of DEEA/H_2O, MAPA/H_2O and DEEA/MAPA (see Tables 2, 3 and 4) were found to be sufficient to predict the ternary system with AARD values 18%, 15% and 2% in activity coefficients of DEEA and MAPA, and the total pressure respectively. It is also clear that the binary interaction parameters for the DEEA/MAPA system are necessary to obtain a good fit for the ternary mixture.

Figure 13. Experimental and predicted activity coefficients for DEEA(1) and MAPA(2) in the DEEA/MAPA/H_2O system at 40^oC (a), 50^oC (b), 60^oC (c), 80^oC (d), 100^oC (e) and 110^oC (f)

Freezing point depression data for ternary system are plotted together with model predictions in Fig. 14. It is interesting to see that the model works well with an AARD= 7.4%. There is a tendency, however, that the model slightly under-predicts the freezing point depression at high amine concentrations. The reasons discussed previously could be used for this case. The freezing point depression of the binary DEEA/H_2O system was larger than for the MAPA/H_2O system. Hence an increasing concentration of DEEA gives a significant effect in increasing the freezing point depression of the ternary system.

To be able to evaluate the volatility of DEEA and MAPA is important for a possible process application of the system. Our results show that even if MAPA in pure form has higher volatility in the whole temperature range investigated, it has very low volatility in aqueous solutions. The activity coefficients for MAPA are very low, in the range 0.05-0.3 at infinite dilution in the temperature range 40-100^{o}C. On the other side DEEA has very high activity coefficient at low concentration, ranging from 12 -24 at infinite dilution. This may constitute a problem for process applications.

Figure 14. Experimental freezing point depression for the ternary DEEA/MAPA/H_2O system at different ratio of DEEA/MAPA

6.5. Termodynamic consistency for all three systems

The directly measured variables in the ebulliometer were P and T while the liquid (x) and vapor (y) compositions were determined by the selected analytical method. It is basically enough to characterize the system from the P-T-x data according to the phase rule and when the collected P-T-x-y are available then the system is over-determined, hence a thermodynamic consistency based on the Gibbs-Duhem equation (Van Ness, 1995) must be fulfilled and can be checked. The parity plots of the measured and calculated model of the activity coefficients (g_i), pressure, composition and the ratio of activity coefficients are shown in Fig. S1, S3 and S3 for the DEEA(1)/H_2O(3), MAPA(2)/H_2O(3) and DEEA(1)/MAPA(3) systems respectively. Overall the measured data were thermodynamically very consistent. However, we observed that a few points could be deemed inconsistent in the lower concentration ranges of DEEA for both the DEEA(1)/H_2O(3) and the DEEA(1)/MAPA(3) systems. For the MAPA(2)/H_2O(3) system, inconsistency can be seen at higher concentrations of MAPA (x> 0.25) as was also reported in the work of Kim et al. (Kim, et al., 2008).

7. Conclusion

New ebulliometric VLE data for the binary DEEA/H_2O and DEEA/MAPA systems and the ternary DEEA/MAPA/H_2O system were generated at different temperatures and concentrations. A combined titration and LCMS technique to quantify the composition of the individual amine mixtures in the

ternary system was successfully carried out in this work. The titration technique was also sufficient to quantify the concentration of DEEA and MAPA in the binary DEEA/MAPA system.

Results show that DEEA is more volatile than some of the commercial solvents such as MEA and MDEA whereas MAPA has the same order of volatility as Pz but is less volatile than MEA. In pure condition MAPA is more volatile than DEEA, while in aqueous solution it is observed that MAPA is much less volatile than DEEA. It is also observed that the activity coefficients for the species in the ternary system are lower than in the corresponding binary mixture.

The six binary UNIQUAC interaction parameters were determined and were able to predict the P-T-x-y, activity coefficients, excess enthalpies and freezing point depressions for the binary and the ternary system. However, it is noted that there is small inconsistency in the water activity coefficients from ebulliometer and freezing point depression measurements.

Notation

A, B, C = Constants
Alk = Alkalinity of solution $(\text{mol} \cdot kg^{-1})$
F = Objective Function
H^E = Excess Enthalpy $(J \cdot mol^{-1})$
M = Molarity of titrant (H_2SO_4) $(\text{mol} \cdot L^{-1})$
n = Number of experiments
P = Pressure (kPa)
r = UNIQUAC volume parameter
q = UNIQUAC surface area parameter
T = Temperature (K)
V = Volume of titrant $(\text{mol} \cdot L^{-1})$
u = UNIQUAC interaction energy parameter (kg)
x = Liquid phase mol fraction
y = Vapor phase mol fraction
w = Amount of solution (kg)

Greek symbols

γ = Activity coefficient (–)
η = Amine ratio was determined by LC-MS (–)
Q^F = Freezing point depression $(°C)$
F = Poynting factor (–)
Ω = Responses

Subscripts

1 = DEEA
2 = MAPA
3 = H_2O
i, j = Components of i, j
Sol = Solution

Superscripts

calc = Calculated by UNIQUAC
exp = Experimental result
° = Temperature independent for the UNIQUAC interaction energy parameter
T = Temperature dependent for the UNIQUAC interaction energy parameter

Acknowledgments

Financial support from the EC 7th Framework Programme through Grant Agreement No: iCap- 24139 and from the CCERT project supported by the Research Council of Norway (NFR 182607), Shell Technology Norway AS, Metso Automation, Det Norske Veritas AS, and Statoil AS is greatly appreciated.

Appendix: Experimental results

Table A.1. Measured saturation pressures of pure DEEA

Table A. 2. Measured saturation pressures of pure MAPA

Table A.3. VLE data for DEEA (1) + H_2O(3) system at different temperatures

Table A.4. VLE data for DEEA (1) + MAPA(2) system at different temperatures.

Table A.5. Ternary VLE data for DEEA (1)+MAPA(2) + H_2O(3) system at different temperatures.

Figure S1. Parity plots of the thermodynamic consistencies for the binary DEEA(1)/H_2O(3) system.

Figure S2. Parity plots of the thermodynamic consistencies for the binary MAPA(2)/H_2O(3) system.

Figure S3. Parity plots of the thermodynamic consistencies for the binary DEEA(1)/MAPA(2) system.

References

Abrams, D. S., and Prausnitz, J. M., 1974, Statistical Thermodynamics of Liquid Mixtures: A New Expression for the Excess Gibbs Energy of Partly or Completely Miscible Systems, AIChE J., 21(1), 116-128.

Antoine, C., 1888, Tensions des Vapeurs; Nouvelle Rrelation Eentre les Tensions et les Températures, Comptes Rendus des Séances de l'Académie des Sciences, 107, 681–684, 778–780, 836–837.

Aronu, U. E., 2011, Amine and Amino Acid Absorbent for CO2 Capture, Ph.D thesis, Norwegian University of Science and Technology, Trondheim, Norway.

Arshad, M. W., Fosbøl, P. L., von Solms, N., and Thomsen, K., 2013, Freezing Point Depressions of Phase Change CO2 Solvent, Accepted in J. Chem. Eng. Data

da Silva, E. F., Lepaumier, H., Grimstvedt, A., Vevelstad, S. J., Einbu, A., Vernstad, K., Svendsen, H. F., and Zahlsen, K., 2012, Understanding 2.Ethanolamine Degradation in Post Combustion CO2 Capture, Ind. Eng. Chem. Res., 51, 13329-12228.

Dow Chemical, 2003, Alkyl Alkanolamines, The Dow Chemical Company Midland, Michigan, USA

Ge, X., and Wang, X., 2009, Calculations of Freezing Point Depression, Boiling Point Elevation, Vapor Pressure and Enthalpies of Vaporization of Electrolyte Solutions by a Modified Three-Characteristic Parameter Correlation Model, J. Solution. Chem., 38, 1097-1117.

Hartono, A., Saeed, M., Ciftja, A. F. and Svendsen, H. F., 2013, Binary and ternary VLE of the 2-Amino-2-methyl-1-propanol (AMP)/ Piperazine (Pz)/ Water system, Chem. Eng. Sci., 91, 151-161

Hertzberg, T and Mejdell, T., 1998, MODFIT for Matlab: Parameter Estimation in a General Nonlinear Multiresponse Model.

Kapteina, S., Slowik, K., Verevkin, S. P., and Heinstz, A., 2005; Vapor Pressures and Vaporization of a Series of Etnaolamines, J. Chem. Eng. Data, 50, 398-402.

Kim, I., 2009, Heat of Reaction and VLE of Post Combustion CO2-Absorbents, Ph.D thesis, Norwegian University of Science and Technology, Trondheim, Norway.

Kim, I., Svendsen, H. F., and Børresen, E., 2008, Ebulliometric Determination of Vapor-Liquid Equilibria for Pure Water, Monoethanolamine, N-Methyldiethanolamine, 3-(Methylamino)-propylamine, and Their Binary and Ternary Solutions, J. Chem. Eng. Data, 53, 2521–2531.

Klepáčová, K., Huttenhuis, P. J. G., Derks, P. W. J., and Versteeg, G. F., 2011, Vapor pressures of several commercially used alkanolamines, J. Chem. Eng. Data, 56, 2242-2248.

Konduru, , P B., Vaidya, P D., and Kenig, E. Y., 2010, Kinetics of Removal of Carbon Dioxide by Aqueous Solutions of N,N-Diethylethanolamine and Piperazine, Environ. Sci. Technol., 44, 2138-2143.

Ku, H. H., 1966, Notes on the Use of Propagation of Error Formulas, NIST Journal of Research, 70(4), 263-273.

Lebrette, L., Maham, Y., Teng, T. T., Hepler, L. G., and Mather, A. E., Volumetric Properties of Aqueous Solutions of Mono, and Diethylethanolamines at Tempearture from 5 to 80C, Thermochimica Acta, 386, 119-126.

Lepaumier, H., Grimstvedt, A., Vernstad, K., Zahlsen, K., and Svendsen, H. F., 2011, Degradation of MMEA at Absorber and Stripper Conditions, Chem. Eng. Scie., 66, 3491-3498.

Mathonat, C., Maham, Y., Mather, A. E., and Hepler, L. G., 1997, Excess Molar Enthalpies of (Water + Monoalkanolamine) Mixtures at 298.15 K and 308.15 K, J. Chem. Eng. Data, 42, 993-995.

Nguyen, T., Hilliard, M., and Rochelle, G. T., 2011, Volatility of aqueous amines in CO_2 capture, Energy Procedia, 4, 1624-1630.

Raynal, L., Alix, P., Bouillon, P. A., Gomez, A., de Nailly, M. F., Jacquin, M., Kittel, J., di Lella, A., Mougin, P., Trapy, J., 2011, The DMX™ process: An original solution for lowering the cost of post-combustion carbon capture, Energy Procedia, 4, 779-786.

Renon, H., and Prausnitz, J. M., 1968, Local Compositions in Thermodynamic Excess Functions for Liquid Mixtures, A.I.Ch.E. Journal, 14(1), 136-144.

Steele, W. V., Chirico, R. D., Knipmeyer, S. E., and Nguyen, A., 2002, Measurements of Vapor Pressure, Heat Capacity, and Density along the Saturation Line for Cyclopropane Aicd, N,N-Diethyethanoalamine, 2,3-Dihydrofuran, 5-Hexen-2-one, Perfluorobutanoic Acid, and 2-Phenylpropionaldehyse, J. Chem. Eng. Data, 47, 715-724.

Thomsen, K., and Rasmussen, P., 1999, Modeling of Vapor-Liquid-Solid Equilibria in Gas - Aqueous electrolyte Systems, Chem. Eng. Sci., 54, 1787-1802.

Vaidya P. D., and Kenig, E. Y., 2009, Untersuchung der CO2-Absorptioskinetik in wässrigen Lösungen von N,N,-Diethylethanolamin und N-Ethylethanolamin, Chemie Ingenieur Technik, 84(4)475-483.

Van Ness, H., 1995, Thermodynamics in the treatment of vapor/liquid equilibrium (VLE) data, Pure & Appl. Chem., 67(6), 859-872.

Vevelstad, S. J., Grimstvedt, A., Elnan, J., da Silva, E. F., and Svendsen, H. F., 2013, Oxidative degradation of 2-ethanolamine; the effect of oxygen concentration and temperature on product formation, Submitted to the International Journal of Greenhouse Gas Control.

Zhang, J., Qiao. J., and Agar, D. W., 2011, Improvement of lipophilic-amine-based thermomorphic biphasic solvent for energy-efficient carbon capture, Energy Procedia, 23, 92-101.

Figures

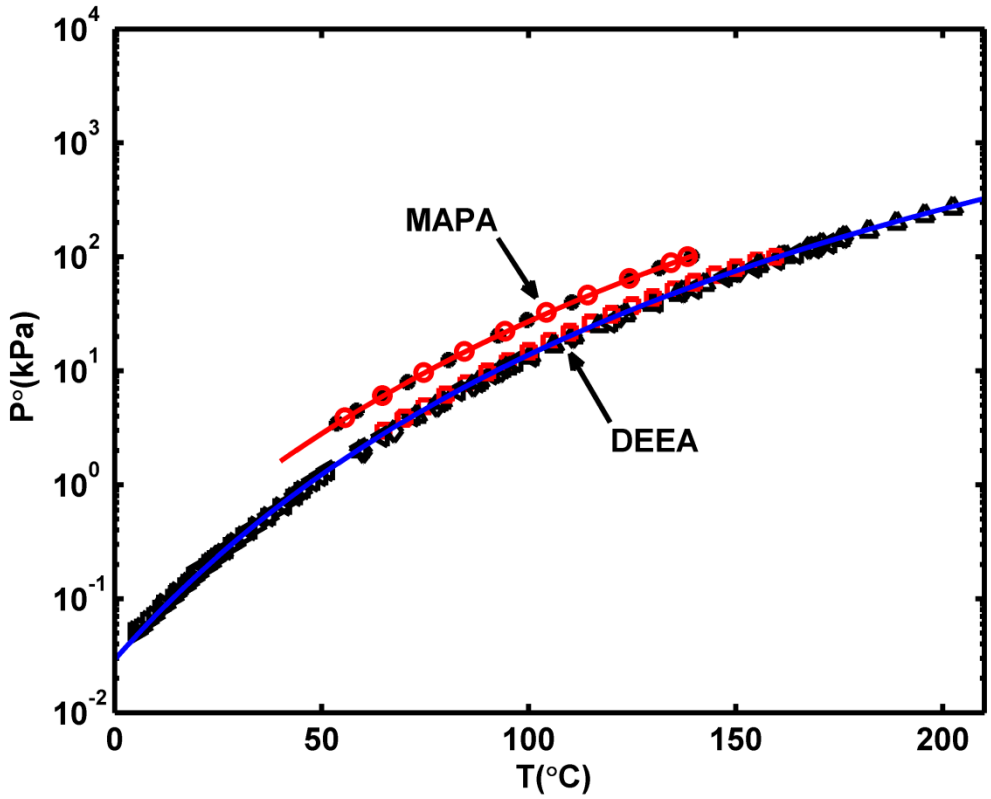

Figure 1. Saturation pressures of pure DEEA(1) and MAPA(2) (○, MAPA (This Work); ✳, MAPA (Kim, et al., 2008); □, DEEA (This Work); ◇, DEEA (Klepáčová, et al., 2011); ▷, DEEA (Kapteina, et al., 2005); △, DEEA (Steele, et al., 2002); ◁, DEEA (Dow Chemical, 2003); Solid lines, Antoine Correlations).

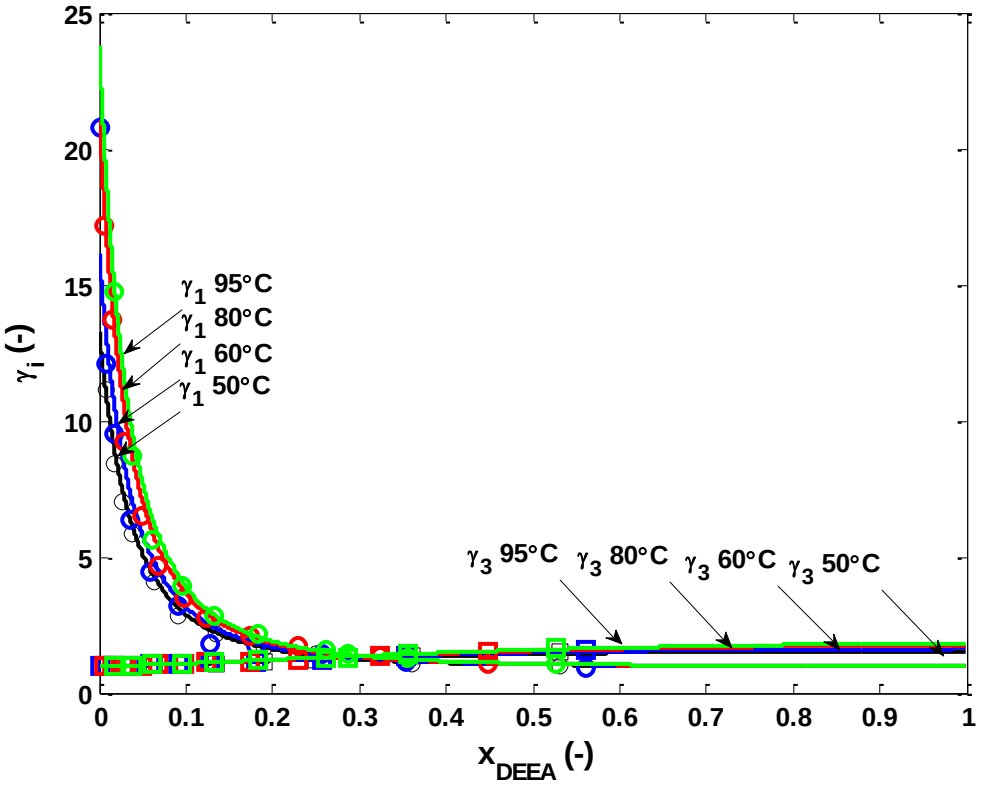

Figure 2. Experimental and predicted activity coefficients for DEEA(1) and H_2O(3) at different concentrations (○, g_1^{Exp} ;□, g_3^{Exp} ; Solid lines, g_1^{Calc} ; Dashed lines, g_3^{Calc} ; Black, 50°C; Blue, 60°C; Red, 80°C and Green, 95°C)

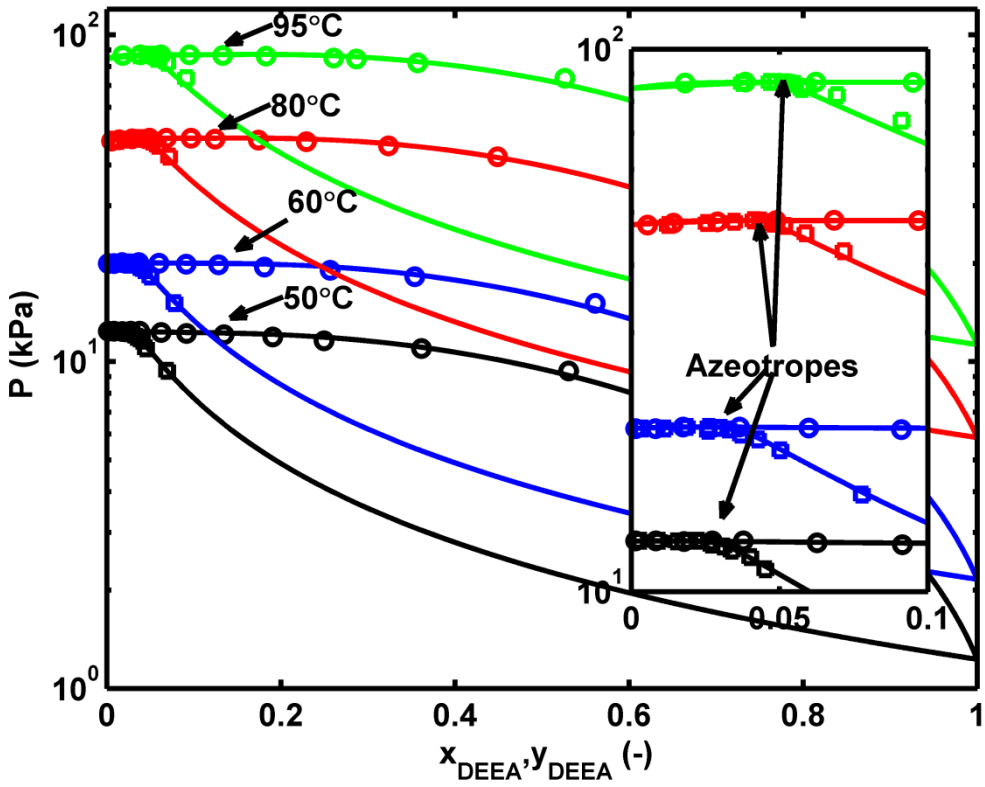

Figure 3. Experimental P-T-x-y data at for DEEA(1)+H_2O(3) system at different temperatures and the predicted models (○ liquid phase, □ vapor phase; Solid lines, model; Black, 50°C; Blue, 60°C; Red, 80°C and Green, 95°C)

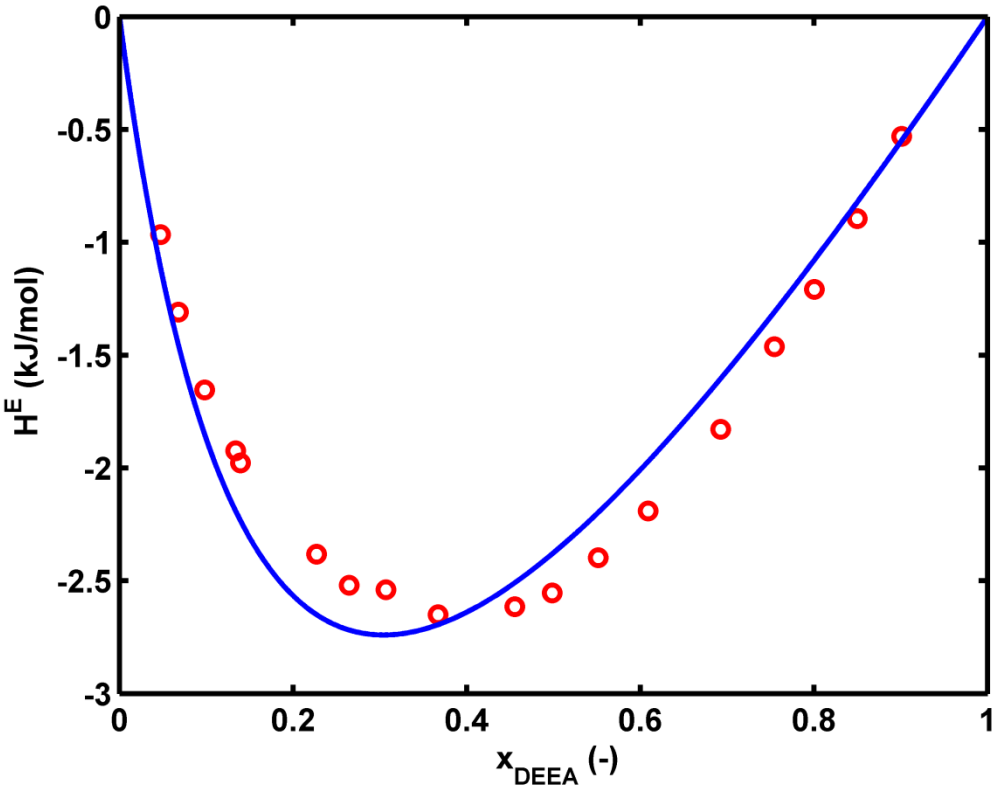

Figure 4. Experimental excess enthalpy of DEEA(1)+H_2O(3) solutions compared to model predictions at 25°C (○, Mathonat, et al., 1997; Solid lines, UNIQUAC)

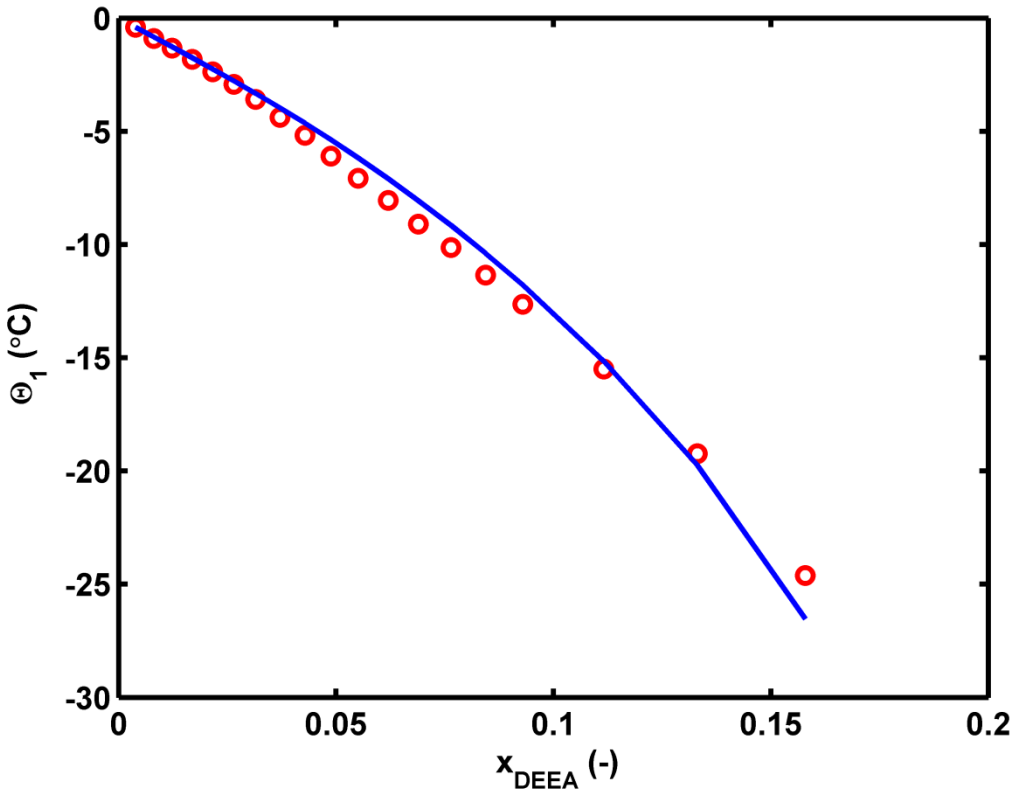

Figure 5. Experimental freezing point depression of DEEA(1) solution and the predicted model (○, Arshad, et al., 2013; Solid line, UNIQUAC)

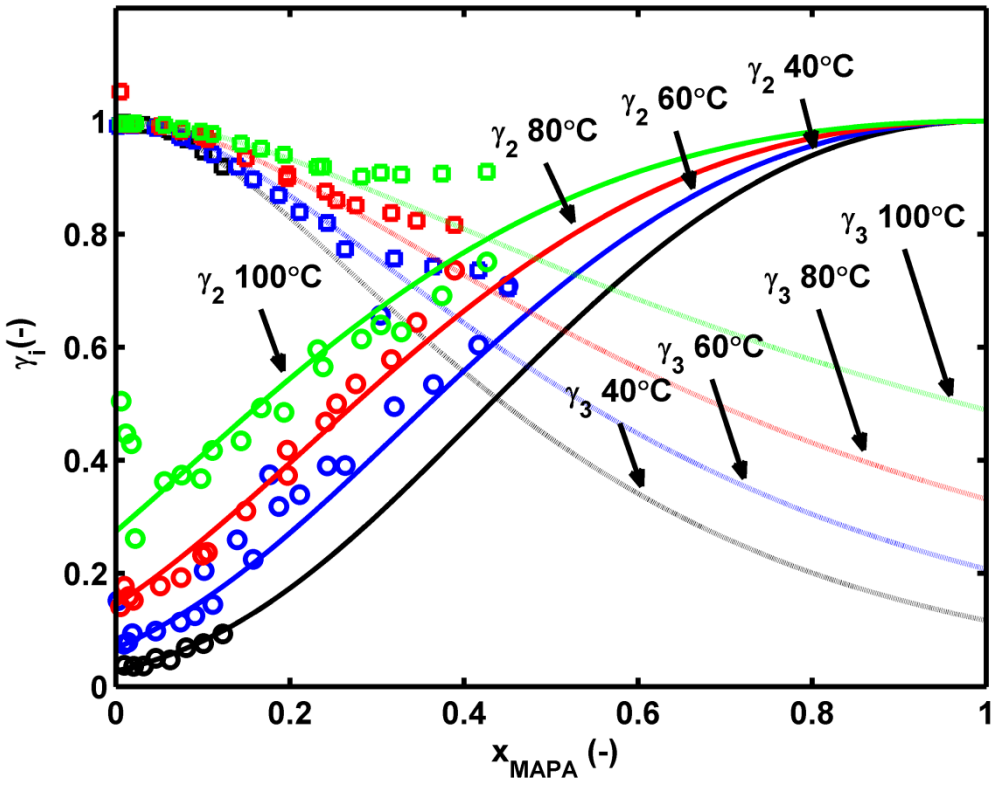

Figure 6. Experimental data (Kim, et al., 2008) and predicted activity coefficients for MAPA(2) and H_2O(3) at different concentrations (○, g_2^{Exp} ;□, g_3^{Exp} ; Solid lines, g_2^{Calc} ; Dashed lines, g_3^{Calc} ; Black, 40°C; Blue, 60°C; Red, 80°C and Green, 100°C)

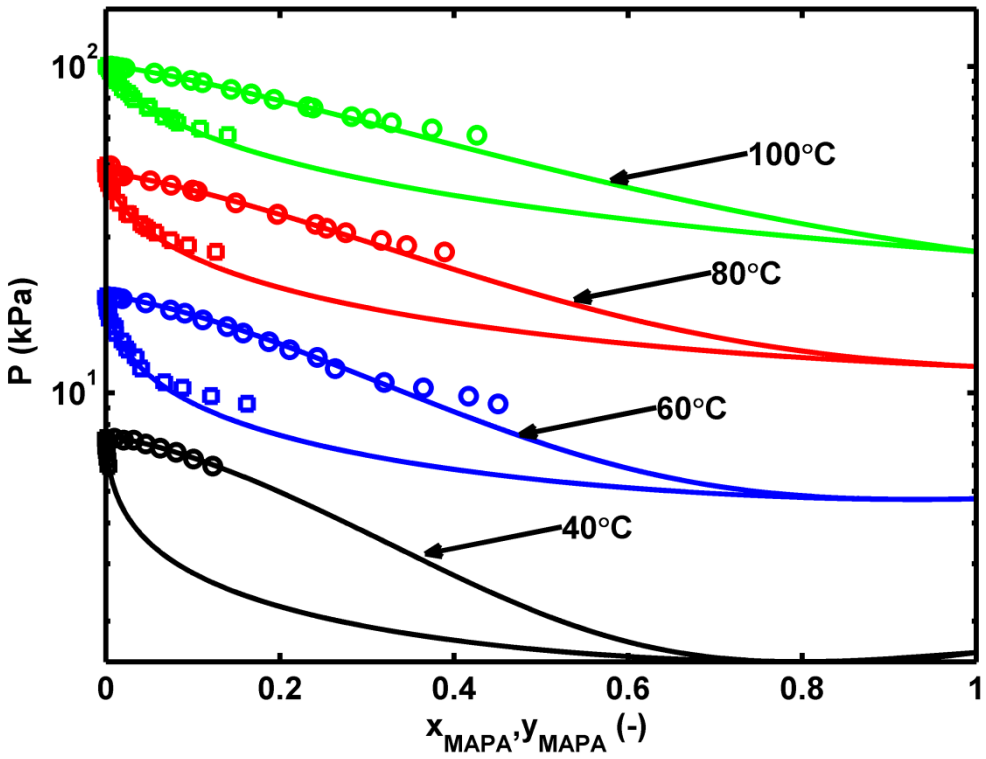

Figure 7. Experimental P-T-x-y data for MAPA(2)+H_2O(3) system at different temperatures and the predicted models (○ liquid phase/□ vapor phase, Kim, et al., 2008; Solid lines, UNIQUAC; Black, 40°C; Blue, 60°C; Red, 80°C and Green, 100°C)

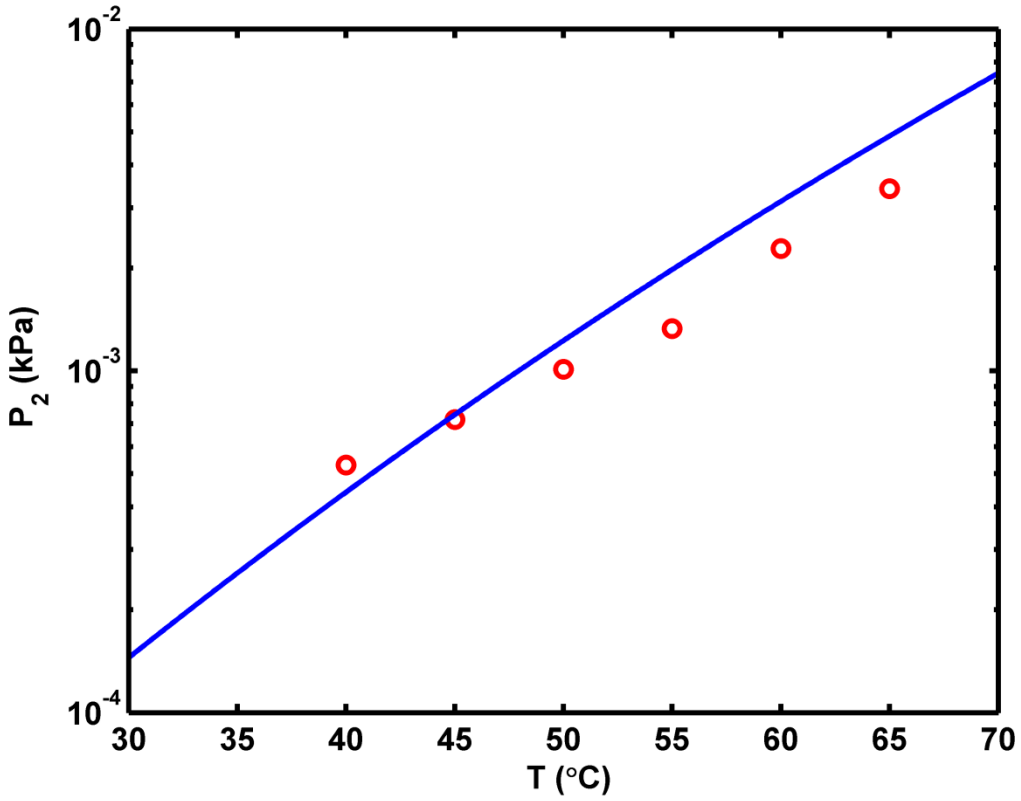

Figure 8. MAPA(2) vapor pressure at 0.5 molality (m) and 40-70°C (○, Nguyen, et al., 2010; Solid line, UNIQUAC)

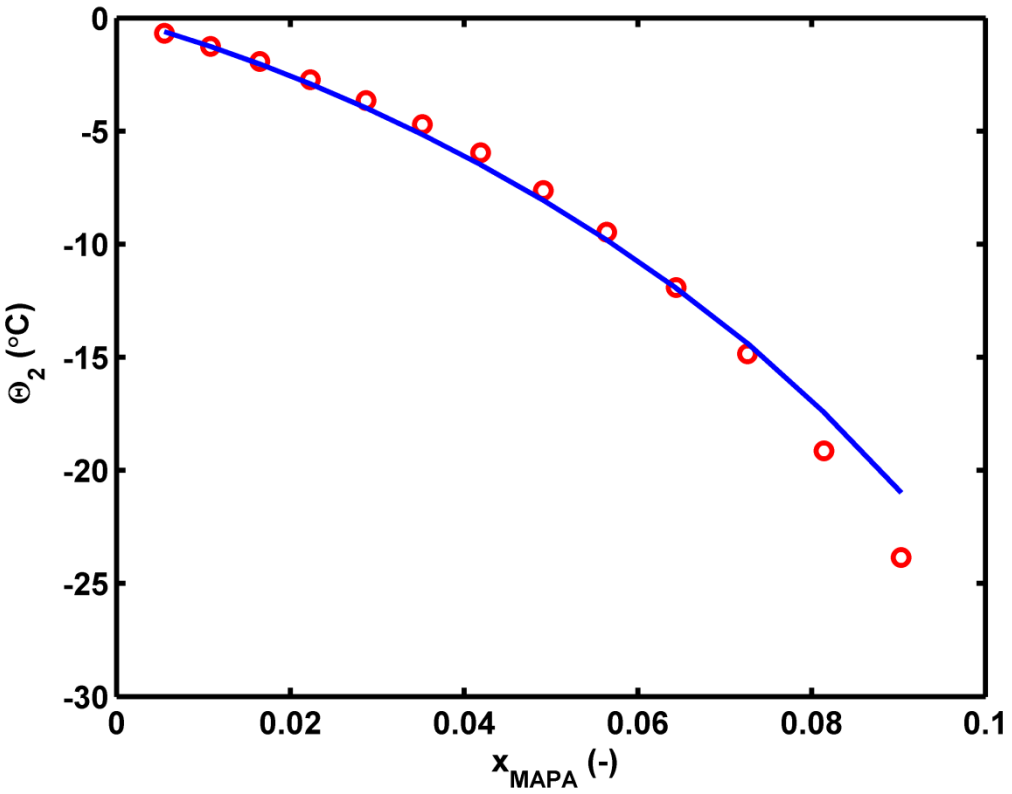

Figure 9. Experimental freezing point depression of MAPA(2) solution and the predicted model (○, Arshad, et al., 2013; Solid line, UNIQUAC)

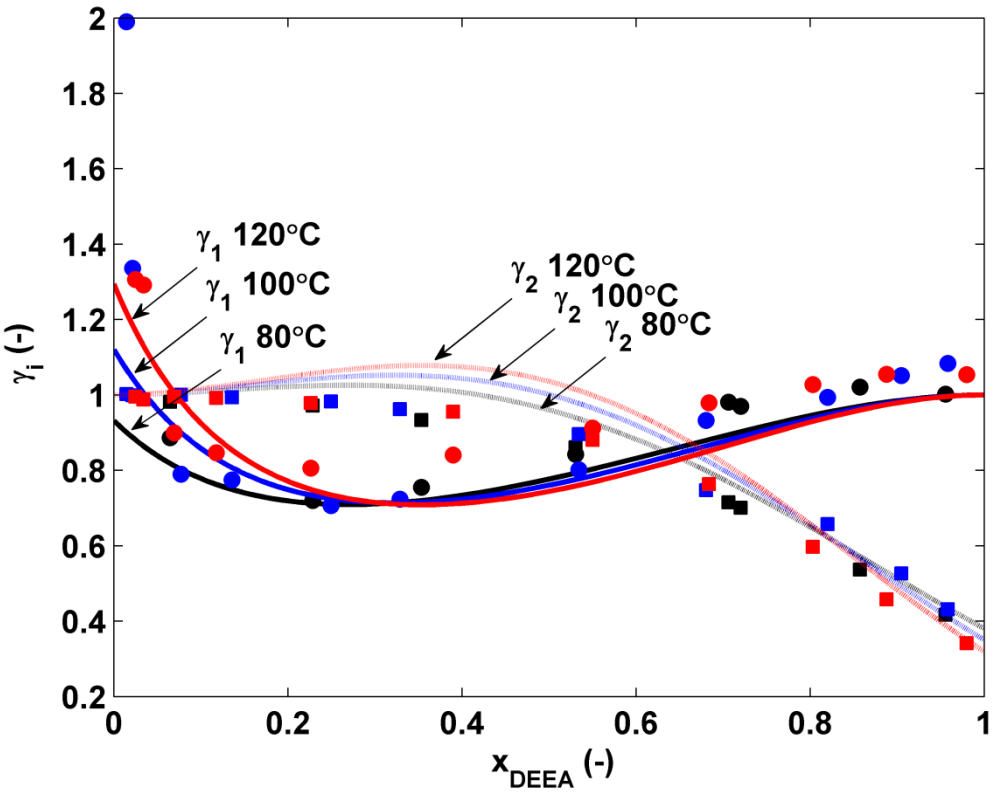

Figure 10. Experimental data and predicted activity coefficients for DEEA(1) and MAPA(2) at different concentrations (○, g_1^{Exp};□, g_2^{Exp}; Solid lines, g_1^{Calc}; Dashed lines, g_2^{Calc}; Black, 80°C; Blue, 100°C; Red, and 120°C)

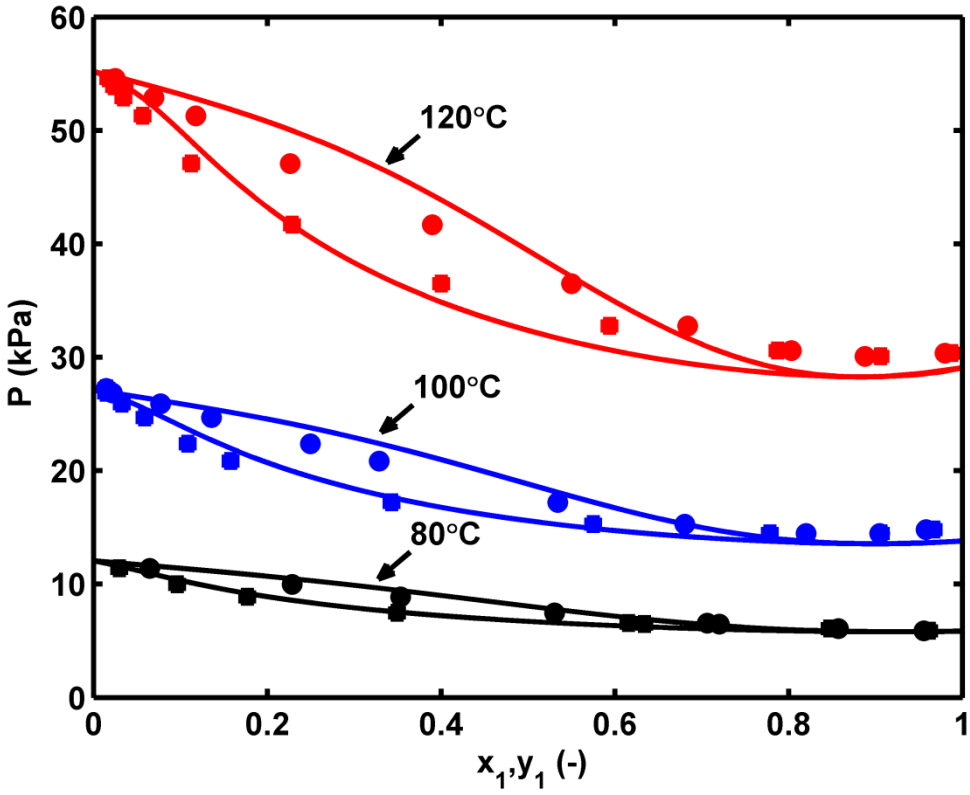

Figure 11. Experimental P-T-x-y data for DEEA(1) and MAPA(2) at different temperatures and the predicted models (● liquid phase/■ vapor phase; Solid lines, UNIQUAC; Black, 80°C; Blue, 100°C; Red, and 120°C)

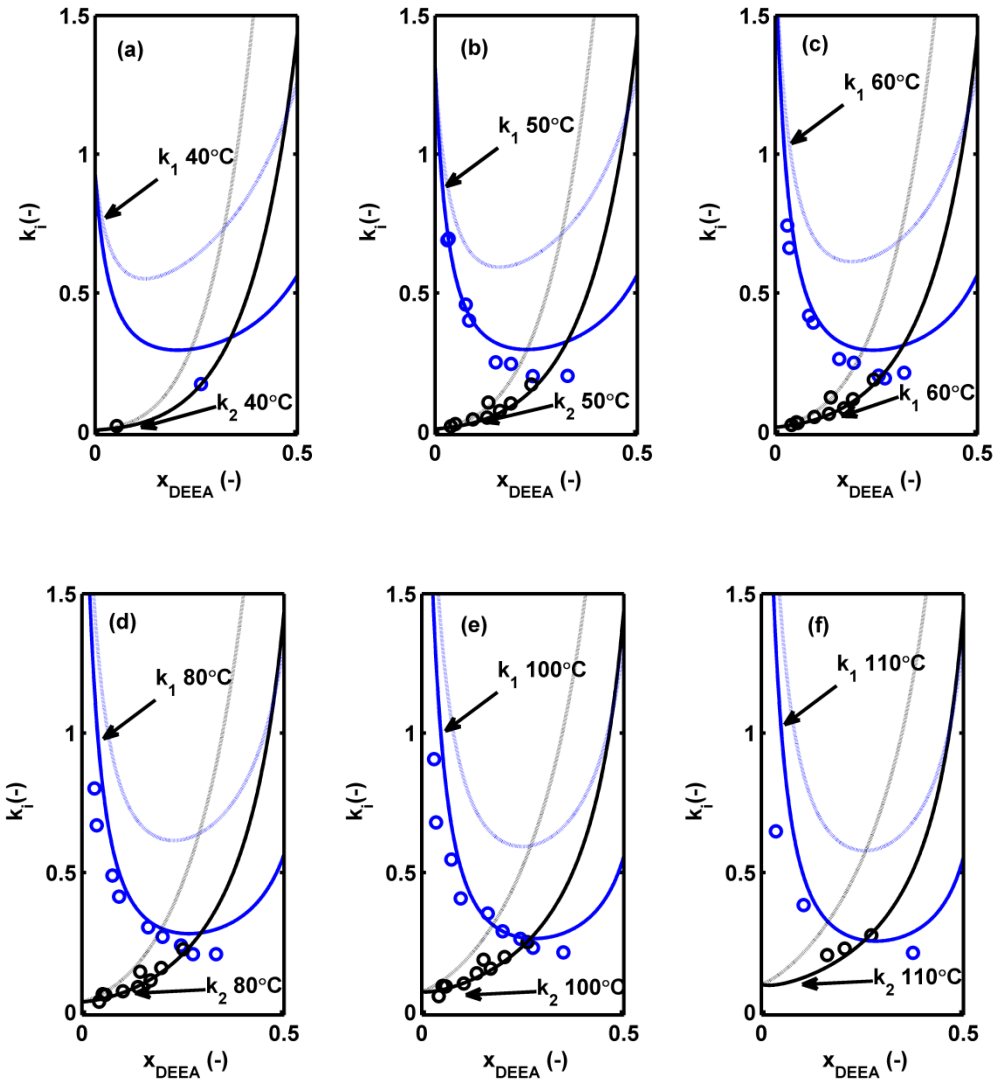

Figure 12. Experimental and predicted k-values for DEEA(1) and MAPA(2) in the DEEA(1)/MAPA(2)/H_2O(3) system at 40°C (a), 50°C (b), 60°C (c), 80°C (d), 100°C (e) and 110°C (f) ($\bigcirc, k_1^{Exp}$; $\bigcirc$, k_2^{Exp}; Solid lines, UNIQUAC with binary DEEA/MAPA interaction parameters; Dashed lines, UNIQUAC without binary DEEA/MAPA interaction parameters).

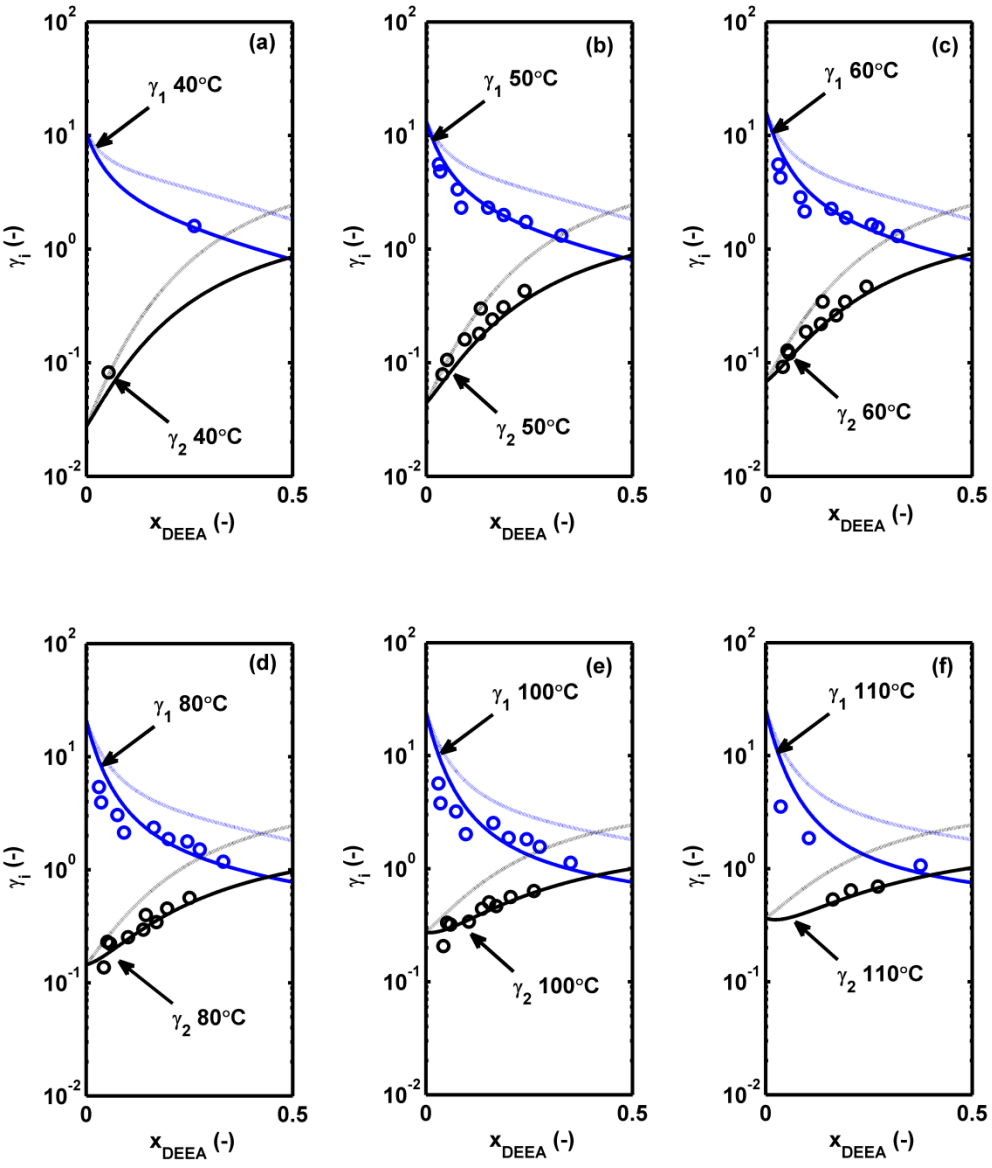

Figure 13. Experimental and predicted activity coefficients for DEEA(1) and MAPA(2) in the DEEA(1)/MAPA(2)/H_2O(3) system at 40°C (a), 50°C (b), 60°C (c), 80°C (d), 100°C (e) and 110°C (f) (○, g_1^{Exp}; ○, g_2^{Exp}; Solid lines, UNIQUAC, with binary DEEA/MAPA interaction parameters; Dashed lines, UNIQUAC without binary interaction of DEEA/MAPA).

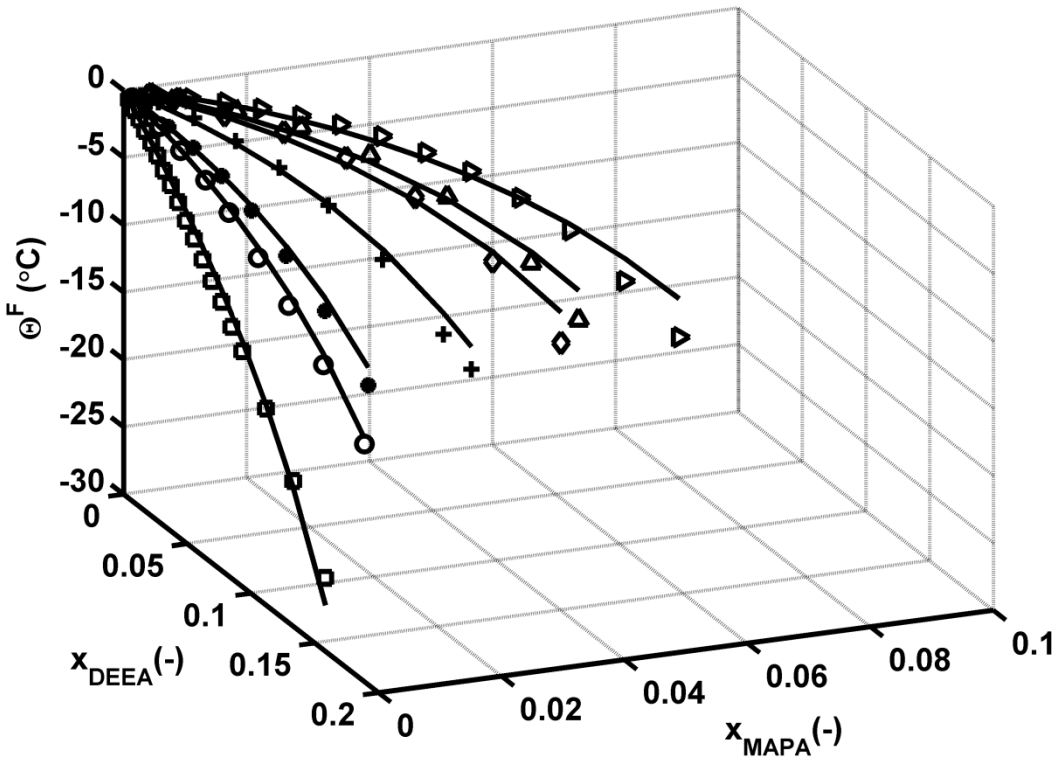

Figure 14. Experimental freezing point depression for the ternary DEEA(1)/MAPA(2)/H_2O(3) system at different DEEA(1)/MAPA(2) ratios (Arshad, et al., 2013) (□, DEEA/0; ○, 5/1; ●, 3/1; +, 1/1; ◊, 1/3; △, 1/5; ▷, 0/MAPA; Solid lines, UNIQUAC)

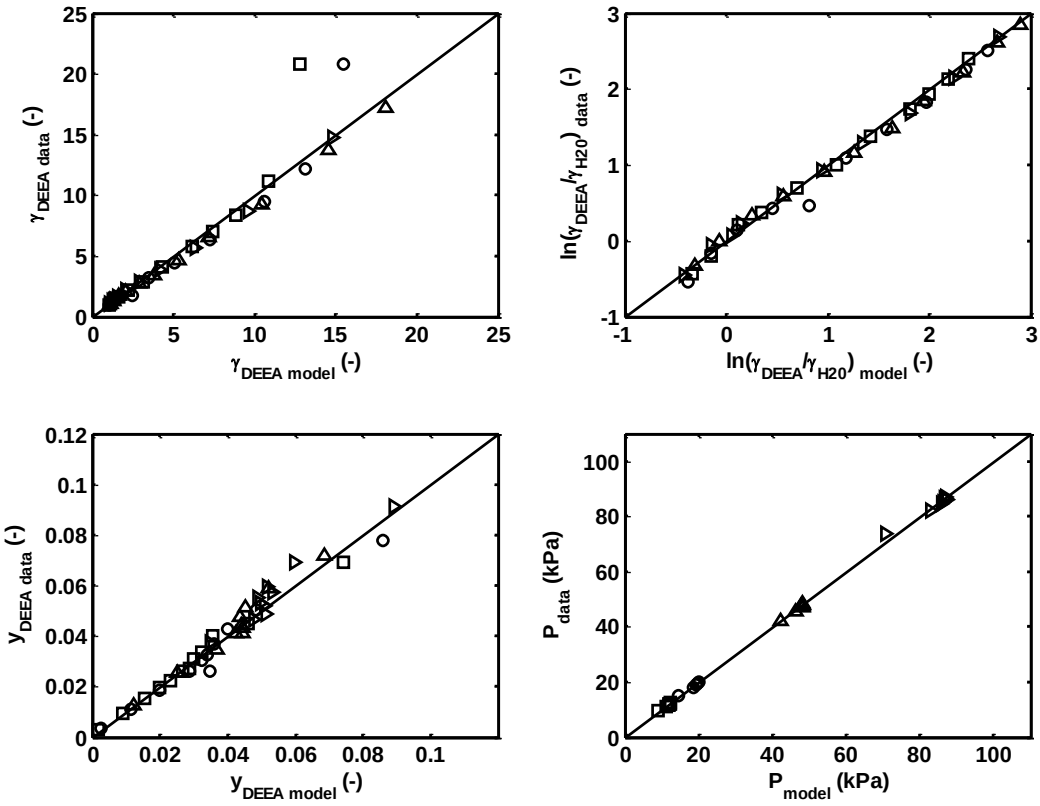

Figure S1. Parity plots of the thermodynamic consistencies for the binary DEEA(1)/H_2O(3) system (○, 50°C ;□, 60°C ;; △, 80°C; ▷, 95°C)

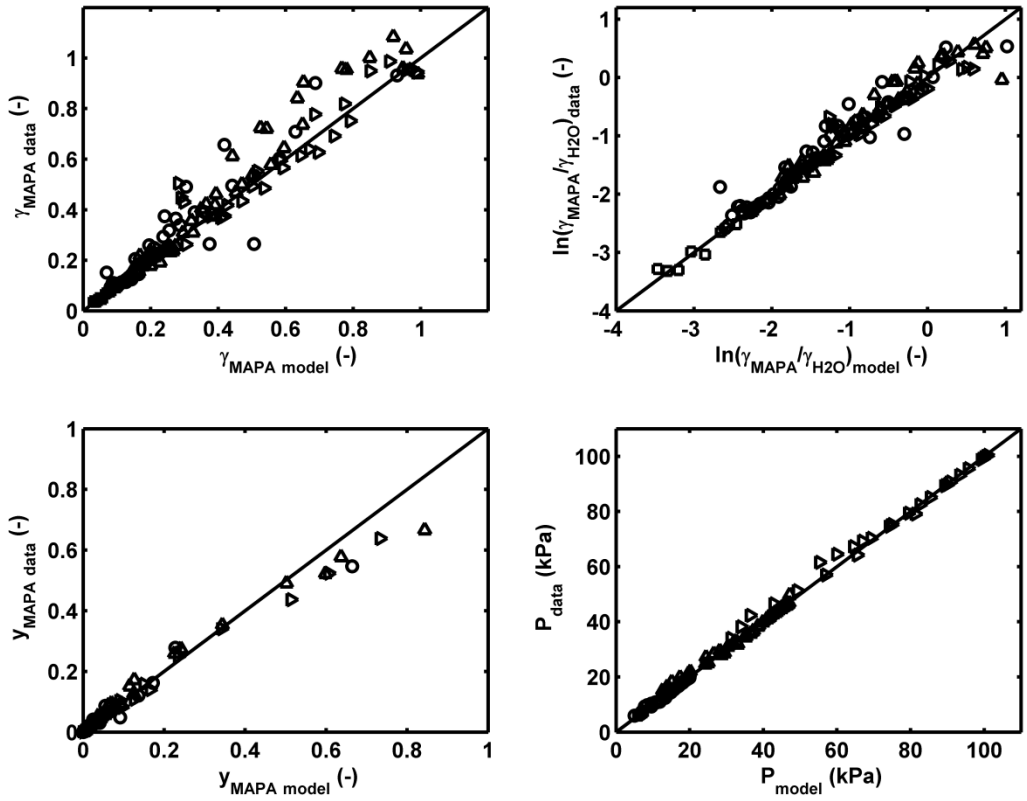

Figure S2. Parity plots of the thermodynamic consistencies for the binary MAPA(2)/H_2O(3) system (○, 40^oC ;□, 60^oC ;; △, 80^oC; ▷, 100^oC)

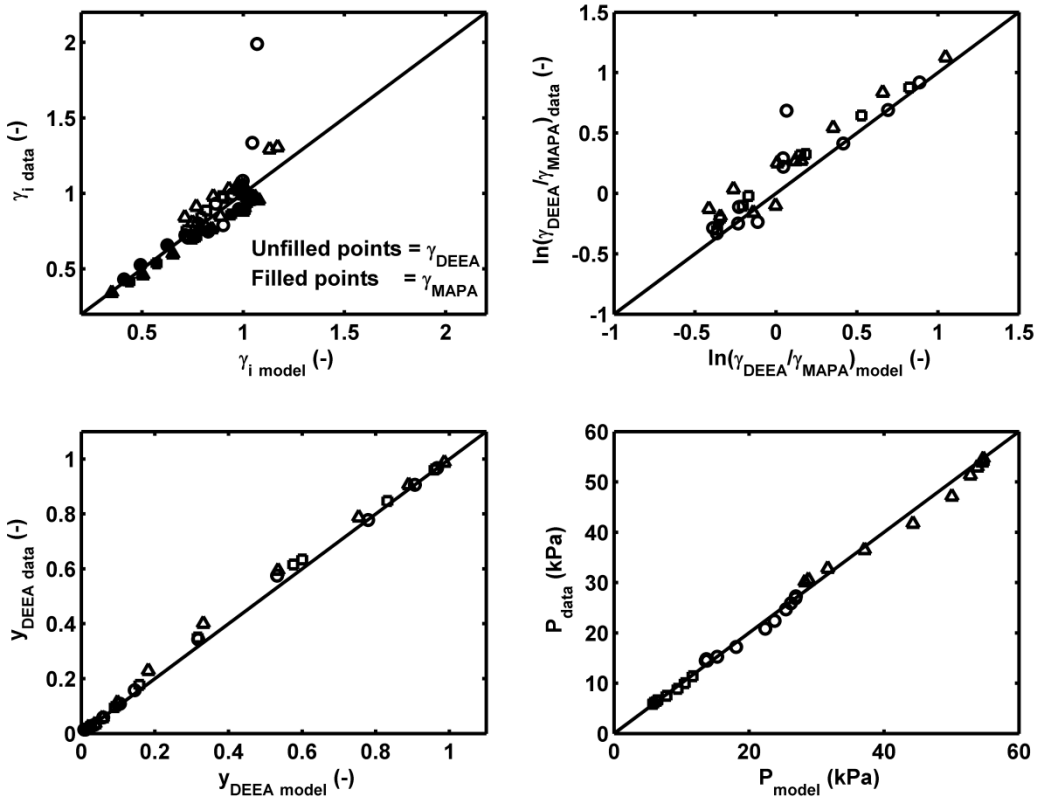

Figure S3. Parity plots of the thermodynamic consistencies for the binary DEEA(1)/MAPA(2) system (○, 80°C ;□,100°C ; △,120°C)

Tables

Table 1. Antoine equation and the obtained parameters for pure DEEA and MAPA

$\ln P_i^{\circ}(kPa) = A - \frac{B}{C + T(^{o}\mathrm{K})}$		
	DEEA	MAPA
A	13.92±0.1	14.86±0.3
B	3198.0±71	3530.43±223
C	-89.9±3	-67.82±9
AARD (%)	4.7	1.7

Table 2. Volume (r) and surface area (q) parameters for the selected systems

Compound	**r**	**q**	**Source**
DEEA	4.59	3.45	This work
MAPA	2.48	3.43	This work
H_2O	0.92	1.44	Abrams and Prausnitz (1974)

Table 3. UNIQUAC interaction energy parameters for $u_{ij} = u_{ij}^{\circ} + u_{ij}^{T} \times (T - 298.15); u_{ij}^{\circ} = u_{ji}^{\circ}$

u_{ij}°	H_2O	DEEA	MAPA
H_2O	0		
DEEA	217.66	-43.88	
MAPA	-274.0	-48.09	225.14

Table 4. UNIQUAC interaction energy parameters for $u_{ij} = u_{ij}^{\circ} + u_{ij}^{T} \times (T - 298.15); u_{ij}^{T} = u_{ji}^{T}$

u_{ij}^{T}	H_2O	DEEA	MAPA
H_2O	0		
DEEA	-1.94	4.12	
MAPA	1.42	-1.53	0.70

Table 5. Absolute average relative deviations (AARD) of model for DEEA(1)+H_2O(3), MAPA(2)+H_2O(3) and DEEA(1)+MAPA(2) .

	DEEA/H_2O		**MAPA/H_2O**		**DEEA/MAPA**	
	Number of points (N)	**AARD (%)**	**Number of points (N)**	**AARD (%)**	**Number of points (N)**	**AARD (%)**
g_i	44	8	62	10	30	9
P_{Sol}	44	1	62	2	30	4
H_{Sol}^{E}	18	9	-	-	-	-
Q_{Sol}^{F}	19	7	13	6	-	-

Appendix: Experimental results

Table A.1. Measured saturation pressures of pure DEEA

t(°C)	P°_{DEEA}(kPa)	t(°C)	P°_{DEEA}(kPa)
64.91	2.9	109.98	22.0
64.97	2.9	115.01	26.5
69.70	3.7	115.02	26.0
70.02	3.9	120.00	31.1
70.05	3.8	120.01	31.6
74.80	4.8	120.04	31.1
74.95	4.8	124.97	36.8
79.84	6.1	125.01	37.5
79.90	6.2	129.96	43.6
79.99	6.1	130.00	43.4
84.98	7.7	130.01	44.1
85.00	7.7	134.99	51.7
89.98	9.6	135.00	50.9
90.00	9.8	139.92	59.1
90.01	9.7	139.98	60.3
94.97	12.1	140.01	59.4
95.05	12.0	144.98	68.9
99.97	14.7	144.99	69.9
100.00	14.9	150.00	79.7
100.08	14.8	150.01	79.5
105.02	17.9	150.01	80.7
105.04	18.2	154.97	91.4
109.90	21.7	154.98	92.5
109.97	21.6	159.53	100.1

Table A. 2. Measured saturation pressures of pure MAPA

t(°C)	P°_{MAPA}(kPa)
55.57	3.9
64.61	6.1
74.57	9.7
84.40	14.9
94.27	22.3
104.23	32.6
114.18	46.5
124.25	65.1
134.31	89.2
138.36	100.7

Table A.3. VLE data for DEEA (1) + H_2O(3) system at different temperatures

t(°C)	P(kPa)	x_1	y_1	$k_1 = y_1/x_1$
49.99	11.0	0.3616	0.0453	0.1252
49.96	9.4	0.5306	0.0694	0.1308
50.00	11.6	0.2496	0.0402	0.1611
50.00	11.9	0.1907	0.0339	0.1777
50.02	12.1	0.1348	0.0312	0.2313
50.00	12.2	0.0914	0.0271	0.2967
50.00	12.3	0.0626	0.0262	0.4191
50.00	12.4	0.0378	0.0226	0.5962
50.00	12.4	0.0273	0.0196	0.7196
50.00	12.4	0.0178	0.0153	0.8635
50.00	12.4	0.0083	0.0094	1.1392
50.00	12.4	0.0015	0.0031	2.1333
60.02	15.1	0.5611	0.0779	0.1388
60.04	18.2	0.3538	0.0503	0.1422
60.03	19.1	0.2567	0.0428	0.1669
59.99	19.5	0.1809	0.0371	0.2049
60.01	19.9	0.0911	0.0328	0.3605
59.99	19.8	0.1283	0.0525	0.4094
59.99	20.0	0.0598	0.0302	0.5052
59.99	20.1	0.0365	0.0262	0.7160
59.99	20.1	0.0175	0.0188	1.0705
60.05	20.0	0.0082	0.0112	1.3742
60.01	20.0	0.0015	0.0036	2.3523
79.99	42.4	0.4489	0.0716	0.1596
79.99	45.8	0.3237	0.0589	0.1819
80.01	47.2	0.2291	0.0516	0.2253
80.01	47.7	0.1742	0.0479	0.2748

79.99	48.0	0.1243	0.0442	0.3558
79.96	48.3	0.0968	0.0434	0.4487
79.99	48.4	0.0684	0.0412	0.6022
79.99	48.3	0.0488	0.0412	0.8446
80.02	48.1	0.0290	0.0347	1.1993
80.02	47.8	0.0142	0.0255	1.7918
79.99	47.4	0.0055	0.0124	2.2681
95.00	73.8	0.5263	0.0912	0.1733
95.00	82.3	0.3571	0.0694	0.1942
95.02	84.4	0.2867	0.0576	0.2008
95.00	85.1	0.2606	0.0596	0.2288
95.01	86.3	0.1828	0.0550	0.3011
95.01	86.7	0.1332	0.0531	0.3990
95.00	86.9	0.0950	0.0517	0.5441
95.01	87.0	0.0622	0.0487	0.7831
94.95	87.0	0.0384	0.0466	1.2151
94.99	86.6	0.0181	0.0373	2.0618

Table A.4. VLE data for DEEA (1) + MAPA(2) system at different temperatures.

t(°C)	P(kPa)	x_1	y_1	$k_1 = y_1/x_1$
79.95	11.39	0.0647	0.0295	0.4551
79.96	9.98	0.2287	0.0965	0.4219
80.08	8.88	0.3535	0.1770	0.5005
79.96	7.48	0.5304	0.3495	0.6590
79.94	6.58	0.7063	0.6158	0.8719
80.09	6.48	0.7202	0.6340	0.8803
80.08	6.08	0.8571	0.8472	0.9885
80.15	5.88	0.9558	0.9619	1.0064
100.10	27.28	0.0146	0.0148	1.0117
99.97	26.88	0.0214	0.0147	0.6858
100.05	25.92	0.0773	0.0326	0.4218
99.94	24.68	0.1356	0.0587	0.4325
99.93	22.38	0.2495	0.1086	0.4351
100.05	20.84	0.3288	0.1580	0.4804
99.97	17.22	0.5342	0.3431	0.6423
100.07	15.29	0.6806	0.5753	0.8452
100.02	14.48	0.8202	0.7784	0.9490
99.95	14.48	0.9047	0.9061	1.0016
99.96	14.81	0.9583	0.9671	1.0092
120.02	54.58	0.0248	0.0173	0.6964
119.97	53.89	0.0341	0.0238	0.6966
119.98	52.89	0.0694	0.0343	0.4941
120.04	51.29	0.1175	0.0565	0.4809
119.99	47.10	0.2262	0.1126	0.4979
119.98	41.69	0.3898	0.2286	0.5863
120.02	36.49	0.5500	0.4001	0.7275
119.98	32.78	0.6838	0.5939	0.8686

120.07	30.58	0.8030	0.7872	0.9803
120.00	30.09	0.8879	0.9058	1.0202
119.96	30.38	0.9798	0.9875	1.0078

Table A.5. Ternary VLE data for DEEA (1)+MAPA(2) + H_2O(3) system at different temperatures.

t(°C)	P(kPa)	x_1	y_1	$k_1 = y_1/x_1$	x_2	y_2	$k_2 = y_2/x_2$
40.02	6.18	0.2618	0.0451	0.1724	0.0536	0.0011	0.0214
49.94	9.90	0.0307	0.0212	0.6911	0.1285	0.0066	0.0511
49.96	8.50	0.0339	0.0236	0.6956	0.1872	0.0191	0.1019
50.02	9.00	0.0759	0.0348	0.4592	0.1602	0.0121	0.0755
50.02	7.10	0.0843	0.0338	0.4010	0.2382	0.0406	0.1703
50.02	11.40	0.1500	0.0376	0.2508	0.0394	0.0008	0.0196
49.98	10.00	0.1879	0.0460	0.2448	0.0934	0.0042	0.0452
50.01	10.60	0.2416	0.0486	0.2013	0.0504	0.0014	0.0282
49.95	8.00	0.3274	0.0661	0.2020	0.1318	0.0139	0.1055
59.94	16.09	0.0300	0.0223	0.7435	0.1329	0.0086	0.0646
60.01	13.90	0.0350	0.0232	0.6644	0.1922	0.0226	0.1174
59.98	14.69	0.0834	0.0349	0.4186	0.1701	0.0144	0.0846
60.05	11.79	0.0939	0.0370	0.3939	0.2439	0.0459	0.1883
59.96	18.59	0.1583	0.0415	0.2624	0.0405	0.0010	0.0235
59.96	16.39	0.1942	0.0483	0.2485	0.0970	0.0052	0.0540
60.03	17.57	0.2560	0.0519	0.2027	0.0522	0.0018	0.0346
59.98	17.31	0.2712	0.0524	0.1934	0.0558	0.0018	0.0331
59.98	13.19	0.3190	0.0680	0.2133	0.1375	0.0171	0.1240
79.97	39.38	0.0308	0.0247	0.8009	0.1384	0.0125	0.0904
80.01	34.57	0.0363	0.0243	0.6705	0.1960	0.0311	0.1585
80.00	36.45	0.0757	0.0371	0.4909	0.1700	0.0194	0.1139
79.96	30.08	0.0917	0.0380	0.4147	0.2504	0.0565	0.2254

79.99	45.39	0.1639	0.0499	0.3046	0.0428	0.0016	0.0364
79.98	40.49	0.1994	0.0539	0.2702	0.1013	0.0076	0.0754
80.02	43.78	0.2448	0.0584	0.2387	0.0514	0.0033	0.0636
80.00	42.70	0.2748	0.0571	0.2080	0.0577	0.0036	0.0628
79.96	33.09	0.3320	0.0691	0.2082	0.1442	0.0209	0.1448
100.00	86.57	0.0302	0.0274	0.9085	0.1357	0.0189	0.1389
100.00	77.28	0.0353	0.0240	0.6799	0.2052	0.0405	0.1972
100.00	81.28	0.0731	0.0400	0.5468	0.1702	0.0266	0.1562
100.00	68.69	0.0963	0.0393	0.4081	0.2615	0.0656	0.2507
99.99	99.20	0.1631	0.0577	0.3540	0.0420	0.0024	0.0567
100.00	89.40	0.2002	0.0581	0.2904	0.1039	0.0107	0.1031
100.01	96.10	0.2438	0.0640	0.2625	0.0512	0.0048	0.0941
100.01	93.78	0.2754	0.0636	0.2310	0.0596	0.0055	0.0928
99.97	72.88	0.3503	0.0750	0.2141	0.1528	0.0287	0.1878
110.02	110.97	0.0361	0.0234	0.6491	0.2062	0.0470	0.2278
109.98	99.00	0.1048	0.0402	0.3833	0.2717	0.0748	0.2754
110.01	102.36	0.3752	0.0798	0.2127	0.1625	0.0333	0.2050